Catal Lett (2013) 143:887–894
DOI 10.1007/s10562-013-1026-2

Oxidative Degradation of Organic Dyes Over Supported Perovskite Oxide $LaFeO_3$/SBA-15 Under Ambient Conditions

Ping Xiao · Jingping Hong · Tao Wang · Xuelian Xu · Yuhong Yuan · Jinlin Li · Junjiang Zhu

Received: 8 January 2013 / Accepted: 16 May 2013 / Published online: 7 June 2013

Abstract Supported perovskite oxide, $LaFeO_3$/SBA-15, is investigated for the first time as catalyst for the oxidation of organic dyes using hydrogen peroxide as oxidant. Characterizations such as XRD, XPS, TEM and N_2 physisorption isotherms indicate that the supported catalyst has typical perovskite $LaFeO_3$ structure, and the ordered mesoporous structure of SBA-15 remains unchanged after the formation of $LaFeO_3$. Catalytic tests indicate that $LaFeO_3$/SBA-15 has large adsorption capacity, good catalytic performances, and wide working pH ranges (from 2 to 10) for the oxidation of dyes, e.g., Rhodamine B. Moreover, the catalyst can be reused for at least four times without appreciable loss in the activity, and no dissolved Fe^{3+} ion could be detected by atomic absorption spectrometry after the reaction, suggesting that $LaFeO_3$/SBA-15 is a very stable and active catalyst for the oxidation of dyes in aqueous solution. Comparative tests on various organic dyes, such as reactive brilliant red X-3B, direct scarlet 4BS, methylene blue and Rhodamine B (RhB), indicate that $LaFeO_3$/SBA-15 is more favorable for RhB oxidation, while considerable activity could also be available for other dyes, potentiating its wide applications for industrial removal of dyes. The excellent catalytic performances of $LaFeO_3$/SBA-15 could be attributed to the synergistic effect between SBA-15 and $LaFeO_3$.

Keywords Perovskite oxide · $LaFeO_3$ · SBA-15 · Organic dyes · Oxidative removal · H_2O_2

1 Introduction

The relationship between industrial activity and environmental pollution is a never-ending topic of our modern society. At the time of producing industrial articles for our daily use, we also release large amounts of industrial wastes that are harmful to the environment and our health. The removal of these industrial wastes by post-treatment, or even by preventing their formation in advance, is a challenging task for the industrial plants, especially with the issue of the more and more strict legislations on the emission of industrial wastes.

In case of factories that use organic dyes as raw materials, e.g., textile mill, they discharge large amounts of wastewater containing unused organic dyes. These organic dyes will undergo chemical as well as biological changes, consume dissolved oxygen, and finally destroy aquatic life [1, 2], if they are discharged to the rivers. The removal of organic dyes by adsorption technology using microporous or mesoporous materials, such as industrial wastes [3], activated clay [4], activated sludge [5], beta-cyclodextrin polymer [6], shale oil ash [7] and SBA-3 [8], as adsorbents has been received great attention over the years. However, this method the dyes are not removed radically and the regeneration of adsorbents need additional steps, consuming extra energy and/or resources. This problem can be resolved if catalytic oxidation technology is used. Catalytic oxidation is an alternative and promising way of removing

Electronic supplementary material The online version of this article (doi:10.1007/s10562-013-1026-2) contains supplementary material, which is available to authorized users.

P. Xiao · J. Hong · T. Wang · X. Xu · Y. Yuan · J. Li · J. Zhu (✉)
Key Laboratory of Catalysis and Materials Science of the State Ethnic Affairs Commission & Ministry of Education, South-central University for Nationalities, No. 708 Minyuan Road, Wuhan 430074, Hubei, China
e-mail: ciaczjj@gmail.com

dyes for industrial plants compared to the physical adsorption, as the dyes would be radically oxidized into H_2O, CO_2, or other small molecules that are harmless to the environment, and the catalyst is able to re-use without extra treatment.

Many types of catalysts have been used for dyes oxidation. The classic Fenton catalyst (dissolved Fe(II) and H_2O_2) [9, 10] is capable of oxidizing organic pollutants into harmless chemicals such as CO_2 and H_2O, but its application is limited by the narrow working pH range ($pH < 4$) [11, 12]. Moreover, the separation and recovery of the iron species from the industrial wastewater is also a big challenge [13]. For this, heterogeneous Fenton systems, e.g. iron oxides [14, 15] and iron-immobilized zeolites [16], have received considerable interest and been investigated. Unlike the homogeneous systems, these solid catalysts could be recuperated by filtration and reused in next runs. However, the oxidation efficiency of these catalysts is low and for better catalytic performance the presence of ultrasonic and/or UV light irradiation is essential, to accelerate the electron transfer at the interface of catalyst and dyes [17]. Thus, to gain industrial application many efforts have been made to synthesize better heterogeneous Fenton-like catalysts exploited under natural conditions without ultrasound or ultraviolet. For example, Luo et al. [18] and Zhang et al. [19] reported that perovskite $BiFeO_3$ and $LaTi_{1-x}Cu_xO_3$ are potential catalysts for oxidative removal of dyes using H_2O_2 as oxidant.

Perovskite-type oxides with ABO_3 structure have attracted great interest in catalysis because of their unique structural features and thermal or hydrothermal stability [20–23]. The A- and/or B-site of ABO_3 can be substituted by many foreign metal cations without destroying the matrix structure, as long as the tolerance factor is in the range of 0.7–1.1 [21, 24]. Thus the oxidation state of B-site cations and/or the amount of oxygen vacancy can be controlled, optimizing the material for special use. However, as the synthesis of perovskite-type oxides usually is carried out at high temperatures, this leads to low surface area and decreases the contact area between the catalyst and the reactant, lowering the catalytic activity. In order to make up this defect, one solution is to synthesize porous or supported perovskite oxides, which have enhanced surface area and possesses porous structure.

In this work, we synthesized supported perovskite oxide, $LaFeO_3$/SBA-15, and investigated its catalytic performances for the oxidation of organic dyes using H_2O_2 as oxidant. $LaFeO_3$ is a heterogeneous Fenton-like catalyst that is active for dyes oxidation, while SBA-15 [25, 26] is an ordered mesoporous material that has the ability to absorb organic dyes. We expect that the combination of $LaFeO_3$ and SBA-15 could show synergistic effect in the oxidation of dyes. Indeed, catalytic results show that $LaFeO_3$/SBA-15 has large capacity and high efficiency for the oxidation of dyes including Rhodamine B, reactive brilliant red X-3B, direct scarlet 4BS and methylene blue (MB), and can be reused for at least four times without appreciable decrease in the activity. Effect of pH and H_2O_2 content on the catalytic performances of $LaFeO_3$/SBA-15 was also investigated.

2 Experimental

2.1 Chemicals

$La(NO_3)_3{\cdot}nH_2O$, $Fe(NO_3)_2{\cdot}9H_2O$, $Cu(NO_3)_2{\cdot}3H_2O$, H_2O_2 (30 %, w/w), polyvinyl alcohol (PVA), Tetraethyl orthosilicate (TEOS), citric acid ($C_6H_8O_7{\cdot}H_2O$), anhydrous alcohol and hydrochloric acid were purchased from Sinopharm Chemical Reagent Co., Ltd. China; Pluronic P123 and Rhodamine B were purchased from Sigma-Aldrich. All the chemicals were used as received.

2.2 Synthesis of $LaFeO_3$/SBA-15

The catalysts were prepared by impregnation method. SBA-15 was first prepared according to a reported protocol [27, 28]: P123 (5 g), de-ionized water (75 g) and 2 M HCl (150 mL) were stirred at 35 °C until the P123 was completely dissolved. Then 30 mL of PVA (1wt %) aqueous solution and 10.5 g of TEOS were added dropwise with stirring. After stirring at 35 °C for 24 h the solution was transferred to an autoclave and aged at 100 °C for 24 h. Subsequently, the sample was filtered, dried at 100 °C for 24 h and calcined in muffle furnace at 550 °C for 6 h with a heating rate of 2 °C/min. Such obtained SBA-15 was used as support to prepare supported perovskite catalysts with the following procedure: $La(NO_3)_3{\cdot}nH_2O$ (0.01 mol), $Fe(NO_3)_3{\cdot}9H_2O$ (0.01 mol), citric acid (0.024 mol), de-ionized water (10 mL) and alcohol (20 mL) were first mixed, and to this solution 2 g of SBA-15 was added. The resulting slurry was stirred and heated to 70 °C until it became gel status. The gel was dried at 100 °C overnight, calcined at 500 °C and 700 °C for 4 h, respectively, with a heating rate of 2 °C/min. The loading of $LaFeO_3$ was calculated to be ca 55 % in weight.

2.3 Characterizations

X-Ray diffraction (XRD) patterns were collected using a Bruker D8 Advance X-ray diffractometer (Cu Kα irradiation). The 2θ angle ranged from 0.5° to 5° and 10° to 80° for small-angle and wide-angle measurements, respectively. X-Ray photoelectron spectroscopy (XPS) data were taken on a Thero Electron Corporation VG Multilab 2000 appratus. The binding energy was calibrated with reference

to the C1s level of carbon at 284.6 eV. Transmission electron microscopy (TEM) images were obtained on a Tecnai G2 20 S-Twin appratus with high-resolution transmission electron microscope (200 kV). N_2 physisorption isotherms were determined at liquid-nitrogen temperature (−196 °C) with an Autosorb-1 apparatus. The sample was degassed at 150 °C overnight before measurement.

2.4 Catalytic Tests

0.1 g of $LaFeO_3$/SBA-15 was first added to 50 mL of dye aqueous solution (0.02 mmol/L) for adsorption. Because of the large adsorption capacity of the catalyst, the adsorption procedure was conducted several times, until reaching adsorption/desorption equilibrium (i.e., no change in the absorbance with the adsorption time). The saturated catalyst was then filtered and put into a fresh dye solution (50 mL, 0.02 mmol/L). After stirring for 30 min, 1 mL of H_2O_2 (30 %, w/w) was added to the solution to start the reaction. Catalytic activity was measured at an interval of 30 min. 4 mL of aliquots were collected by filtration and the absorbance was measured at 550 nm using a spectrophotometer (Model: 722E, Shanghai Spectrum Instruments, China). In the study of the effect of pH values, the pH was adjusted by adding H_2SO_4 or NaOH to the solution. The concentration of dyes before and after reaction was calibrated using a standard concentration versus absorbance curve made by external standard method. The oxidation activity was calculated by the following formula:

$$\%\, conversion = \frac{C_0 - C_A}{C_0} \times 100$$

where C_0 and C_A represent the concentration of dyes before and after reaction, respectively.

3 Results and Discussion

Figure 1A shows the XRD patterns of samples measured at small angles. Both SBA-15 and $LaFeO_3$/SBA-15 show three diffraction peaks that are assignable to the (100) (110) and (200) face of SBA-15, suggesting that the loading of $LaFeO_3$ does not destroy the ordered porous structure of SBA-15. The peak intensity of $LaFeO_3$/SBA-15 is significantly attenuated compared to that of SBA-15, which could be due to the partial blocking of pores by $LaFeO_3$ species, resulting in decrease in the long-range order of the channels of SBA-15 [29–31]. Also, it is noticed that the diffraction peak of $LaFeO_3$/SBA-15 is shifted to higher angles. According to the Bragg's law: $2d\sin\theta = n\lambda$, the increase in the diffraction angle (θ) leads to a decrease in the interplanar spacing (d), which means that the unit cell of SBA-15 was shrunk after the formation of $LaFeO_3$. The reason could be that the $LaFeO_3$/SBA-15 undergone an additional hydrolyzation and calcination step during the synthesis process.

Figure 1B shows the XRD patterns of samples measured at wide angles. The diffraction patterns of SBA-15 were not measured at this time as it is an amorphous material that shows no defined diffraction peak in the wide-angle XRD patterns. In order to index the diffraction peaks and confirm the structure of the catalyst, we prepared a bulk $LaFeO_3$ perovskite with the same procedure except the use of SBA-15, and its XRD patterns are presented in Fig. 1B. The predominant peaks of $LaFeO_3$/SBA-15 appear almost at the same position as those of bulk $LaFeO_3$, confirming that the catalyst supported on SBA-15 is in $LaFeO_3$ perovskite structure. By referring to the standard PDF card of perovskite $LaFeO_3$, we found that all the diffraction peaks are attributable to $LaFeO_3$ and no peak assignable to La_2O_3 or Fe_2O_3 appears. The peak intensity of $LaFeO_3$/SBA-15 is attenuated compared to that of $LaFeO_3$, which could be that the $LaFeO_3$ on SBA-15 has poorer crystalline, or that it is highly dispersed and has smaller particle size than the bulk one.

Figure 2A presents the N_2 physisorption isotherms for SBA-15 and $LaFeO_3$/SBA-15. Both show a type H1 hysteresis loop corresponding to an ordered mesoporous structure, confirming that the SBA-15 structure is not destroyed after the formation of $LaFeO_3$, in line with the results observed from XRD measurements. However, the surface area, pore volume and pore size (Fig. 2B) of SBA-15 are significantly decreased after the formation of $LaFeO_3$. The reason could be that some of $LaFeO_3$ block the pores, or are formed on the inner pore walls of SBA-15, decreasing the surface area and pore size, or that the unit cell of SBA-15 was shrank during the impregnation and calcination steps of $LaFeO_3$. Nevertheless, both XRD and N_2 physisorption measurements indicate that the SBA-15 structure is maintained and $LaFeO_3$ is successfully synthesized and formed on SBA-15.

TEM image confirms that the ordered mesoporous structure of SBA-15 is maintained after the formation of $LaFeO_3$, Fig. 3. However, it seems that some amounts of amorphous non-ordered silica are formed, as a layer of thin film appears on the surface. The reason is attributed to the extra treatments on SBA-15 during the synthesis of $LaFeO_3$ in aqueous solution, as suggested by Galarneau et al. [32] Besides, a large amount of particles, with particle size of 10–20 nm are observed on the surface, which suggests that $LaFeO_3$ is present in nanoparticle form and is well dispersed on SBA-15, explaining why $LaFeO_3$/SBA-15 shows attenuated peak intensity compared to the bulk $LaFeO_3$, as observed in the wide-angle XRD patterns.

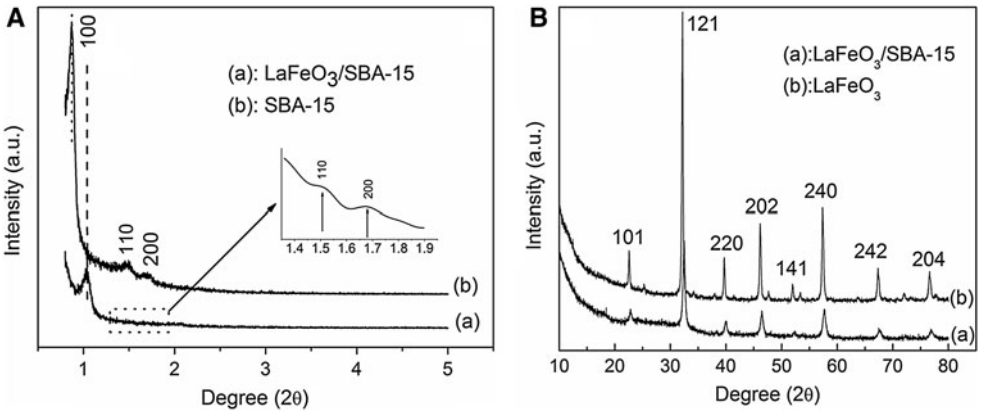

Fig. 1 (**A**) Small-angle XRD patterns for SBA-15 and $LaFeO_3$/SBA-15; (**B**)wide-angle XRD patterns for $LaFeO_3$/SBA-15 and $LaFeO_3$

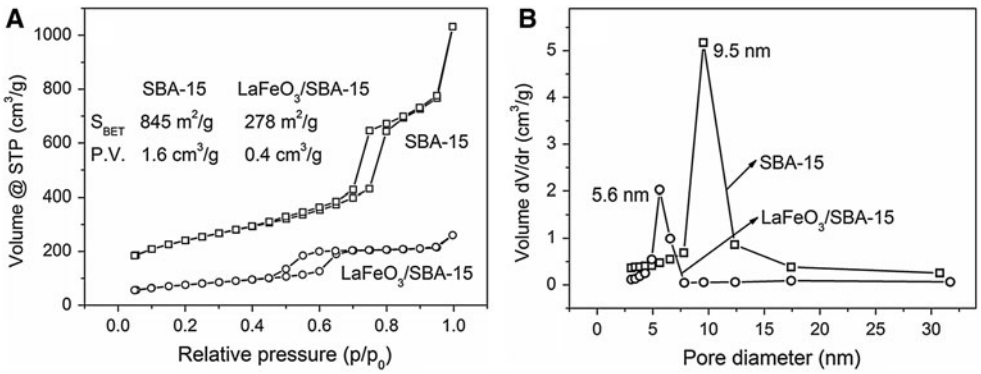

Fig. 2 (**A**) N_2 physisorption isotherms for SBA-15 and $LaFeO_3$/SBA-15 ("S_{BET}" means the surface area measured by BET method; "P.V." means the pore volume); (**B**) The corresponding pore size distribution for SBA-15 and $LaFeO_3$/SBA-15, calculated by BJH method using the adsorption branch

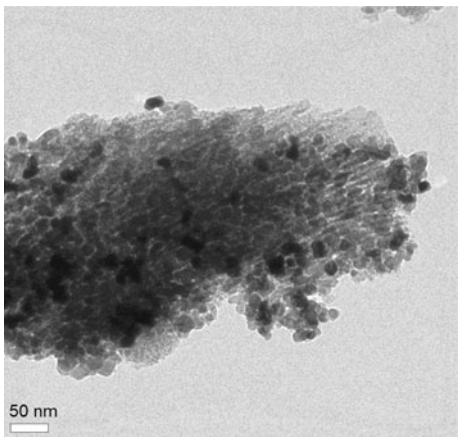

Fig. 3 TEM image for $LaFeO_3$/SBA-15

The oxidation state of principal elements of $LaFeO_3$ nanoparticles on SBA-15 surface was analyzed and determined by XPS measurements. The XPS spectra for La 3d, Fe 2p and O 1s are depicted in Fig. 4. For La 3d and Fe 2p, the peak positions of La $3d_{5/2}$ and Fe $2p_{3/2}$ are located at 834.5 eV and 710.7 eV, respectively. By comparing with the data reported in the handbook of the XPS instrument and those in the literatures [33–36], it is inferred that the main chemical valences of La and Fe are in +3 oxidation state. For O 1s, the XPS spectrum could be deconvolved into two peaks using the Origin software by Gaussian rule. According to literatures [37, 38], the major one at 532.0 eV is attributable to chemically adsorbed oxygen species on the oxygen vacancies, and the shoulder one at 529.6 eV is to lattice oxygen O^{2-}. From the peak area of these two oxygen species, it can be concluded that there are a large amount of adsorbed oxygen on the catalyst. That is, the $LaFeO_3$/SBA-15 prepared by impregnation method contains a lot of oxygen vacancy, which is accepted to be an important parameter influencing the catalytic performances of catalyst in oxidation reactions.

Screening tests were performed on a series of bulk $LaMO_3$ (M = Fe, Co, Ni, Cu) for Rhodamine B (RhB) oxidation. Results in Fig. 5 show that $LaFeO_3$ and $LaCuO_3$ exhibit better activity for RhB degradation than $LaCO_3$ and $LaNiO_3$. The low activity of $LaCO_3$ and $LaNiO_3$ could be due to the rapid decomposition of H_2O_2 on them, leading to the hard production of OH radicals [39]. Adsorption measurements show that all the $LaMO_3$ catalysts exhibit negligible capacity for RhB adsorption due to their low surface area (<10 m^2/g) and non-porous structure. In this work, the $LaFeO_3$ catalyst was used for primary investigation, in order to compare the Fenton-like catalysts reported in literature. Also, because iron is cheaper than copper, this makes $LaFeO_3$ a more potential catalyst for industrial use.

In order to increase the surface area of $LaFeO_3$ and enhance the contact area between $LaFeO_3$ and RhB, we attempted to synthesize nanoscaled $LaFeO_3$ particles by

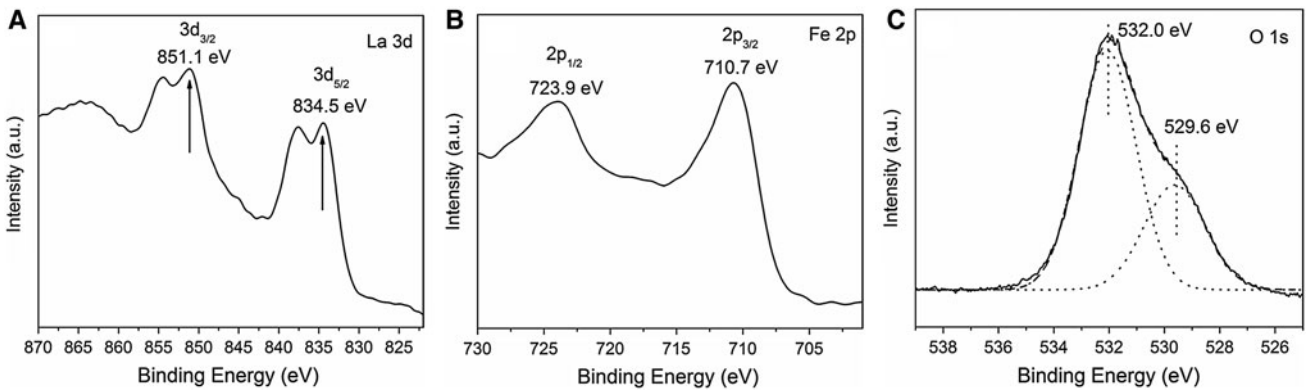

Fig. 4 XPS spectra of (**A**) La 3d, (**B**) Fe 2p and (**C**) O 1s core levels for $LaFeO_3$/SBA-15

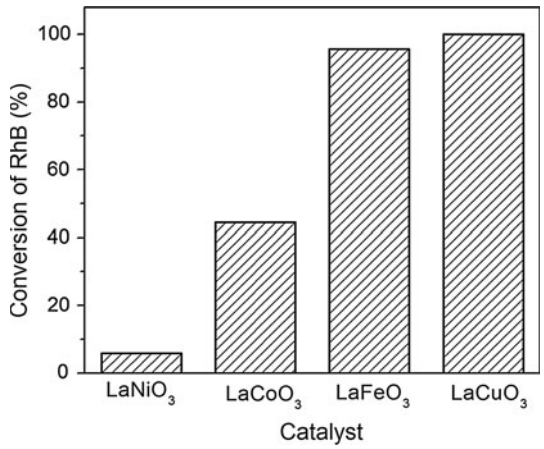

Fig. 5 Degradation activity of the series investigated $LaMO_3$ catalysts for RhB oxidation using H_2O_2 as oxidant. Reaction conditions: 0.1 g catalyst; 1 mL H_2O_2 (30 %, w/w); 50 mL RhB (0.02 mmol/L)

depositing it onto a high-surface-area, mesoporous SBA-15 material [25, 26], which is regarded to be one of the most widely used supports for heterogeneous catalysts. Also, it has been reported that SBA-15 is a good absorbent for dyes adsorption [40, 41]. The capacity of SBA-15, as well as that of $LaFeO_3$/SBA-15, for RhB adsorption is measured by impregnating the sample in 50 mL of RhB aqueous solution (0.02 mmol/L) for several times until no change in the absorbance of the RhB solution is observed. The maximum amount of RhB adsorbed on SBA-15 and $LaFeO_3$/SBA-15 was measured to be 0.017 and 0.013 mmol/g, respectively. By referring to the textural properties shown in Fig. 2, it is surprised to find that although SBA-15 possesses far larger surface area and pore volume than $LaFeO_3$/SBA-15, the capacity of them for RhB adsorption is almost similar. Considering that $LaFeO_3$ can catalyze the RhB oxidation and there has lots of adsorbed oxygen on the surface (see XPS results) that could be acting as oxidant, we inferred that the large capacity of $LaFeO_3$/SBA-15 for RhB adsorption is contributed from two parts: one is from the amount of physically adsorbed RhB, and the other is due to the degradation of RhB that were oxidized by the surface adsorbed oxygen.

Catalytic tests were carried out after the adsorption of RhB on $LaFeO_3$/SBA-15 reaches equilibrium. Namely, the saturated $LaFeO_3$/SBA-15 was filtered and then put into a new batch of 50 mL RhB solution (0.02 mmol/L). After stirring for 30 min 1 mL of H_2O_2 (30 %, w/w) was added to start the reaction. Figure 6A presents the conversion of RhB measured at different conditions. It seems that the activity of supported $LaFeO_3$/SBA-15 is lower than that of bulk $LaFeO_3$ at the initial 100 min. However, it should be noticed that (a) the loading of $LaFeO_3$ on SBA-15 is 55 % in weight, that is, the actual amount of $LaFeO_3$ participating in the catalytic reaction is 0.055 g for $LaFeO_3$/SBA-15, while that for bulk $LaFeO_3$ is 0.1 g. Therefore, considering that SBA-15 has no contribution to the reaction (Figure S1), it can be inferred that the $LaFeO_3$ supported on SBA-15 is more efficiency for RhB oxidation than the bulk one; (b) RhB was adsorbed on $LaFeO_3$/SBA-15 at the adsorption step (before the catalytic test), while none was on bulk $LaFeO_3$ as indicated above. This means that the total amount of RhB converted over $LaFeO_3$/SBA-15 contains both the pre-adsorbed RhB and those in the solution, while that on bulk $LaFeO_3$ contains only the RhB in the solution. In other words, the degradation activity shown in Fig. 6A, represents not the actual ability of the catalysts to RhB oxidation, but the apparent conversion measured from the solution (The conversion of RhB that were pre-adsorbed on the catalyst cannot be embodied in this measurement). Consequently, it is concluded that $LaFeO_3$/SBA-15 is more efficient than $LaFeO_3$ in catalyzing RhB oxidation. The reason could be that, on one hand, SBA-15 has large capacity for RhB adsorption, and on the other hand, $LaFeO_3$ is existing in nanoparticle form with more active sites exposed. As a synergistic effect, the possiblity of RhB reacting with H_2O_2 on the surface of $LaFeO_3$/SBA-15 increases, accelerating the reaction rate.

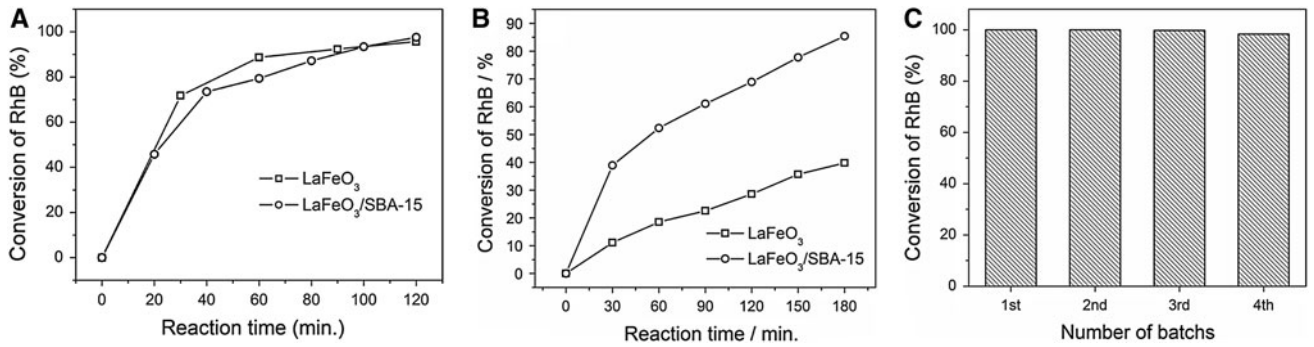

Fig. 6 Degradation activity of $LaFeO_3$/SBA-15 and $LaFeO_3$ for RhB oxidation as a function of reaction time, with weight ratio of RhB to catalyst at (**A**) 0.0048 and (**B**) 0.08; (**C**) Long-term stability of $LaFeO_3$/SBA-15 catalyst for RhB oxidation. Reaction condition: weight ratio of RhB to catalyst is 0.0048; 120 min

In order to justify the superiority of $LaFeO_3$/SBA-15 (v.s. bulk $LaFeO_3$) in catalyzing RhB oxidation, we performed additonal experiments by increasing the weight ratio of RhB to catalyst, from 0.0048 to 0.08. Note: this time the $LaFeO_3$/SBA-15 sample was also undergone an adsorption procedure before the catalytic tests, as described above. The degradation activity for RhB measured under this condition is presented in Fig. 6B, showing that the catalytic performances of $LaFeO_3$/SBA-15 is indeed largely improved compared to that of bulk $LaFeO_3$. This result also implies that $LaFeO_3$/SBA-15 has strong ability to oxidize high-concentration RhB solution.

Stability of $LaFeO_3$/SBA-15 for RhB oxidation was tested to check if the catalyst could be cycled for industrial application. After the reaction, the catalysts were filtered, dried in an oven at 100 °C for several hours, and then put to a new batch of RhB solution, with the same procedure as that for the fresh catalyst. The amount of catalyst in each run was balanced to 0.1 g by adding a few amount of used catalysts that were obtained from parallel experiments. Figure 6C shows the oxidation activity measured at 120 min from different cycles. No appreciable loss in the activity is observed even after four cycles, indicating that the $LaFeO_3$/SBA-15 is stable and has good reusability for RhB oxidation. XRD patterns also confirm that the structure of $LaFeO_3$/SBA-15 is not destroyed even after the catalyst was cycled for four times (Figure S3).

Since the wastewater discharged from different types of industrial plants may have a wide range of pH values, which is a crucial parameter influencing the activity of Fenton-like catalysts for RhB oxidation, we investigated the effect of pH value on the catalytic performances of $LaFeO_3$/SBA-15 for RhB oxidation. The pH value of RhB solution after the addition of 1 mL H_2O_2 is measured to be 5.56, and a desired pH value is adjusted by adding 2 M H_2SO_4 or NaOH to the solution. Figure 7A shows the change of oxidation activity as a function of pH value, measured at reaction time of 100 min. Only a small change in the activity is observed and the activity remains above 93 % throughout the pH ranges, from 2.28 to 10.26, indicating that the catalyst has strong resistance to pH in catalyzing RhB oxidation. Nevertheless, there has a trend that the activity decreases at pH > 9.0, indicating that high pH value would restrain or even block the the reaction to proceed. This is in accordance to the phenomenon observed elsewhere [19].

Effect of H_2O_2 dosage on the degradation activity of $LaFeO_3$/SBA-15 for RhB oxidation was also investigated, with the aim of optimizing the H_2O_2 amount used for the reaction. Figure 7B shows the change in the degradation

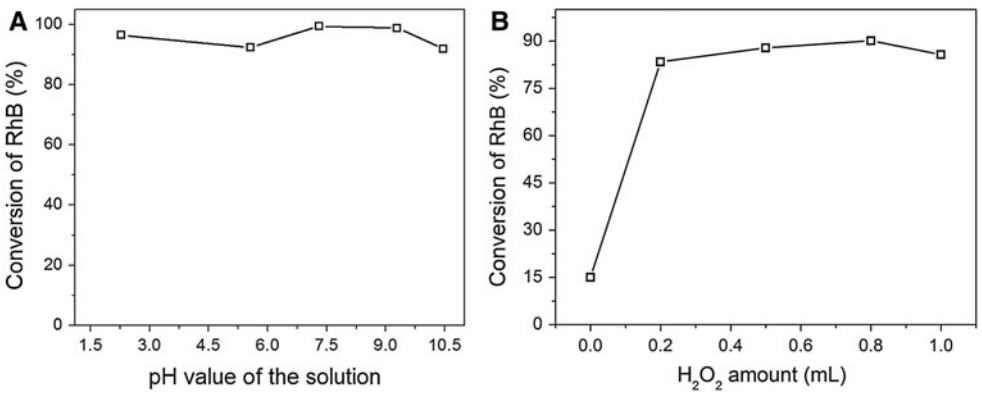

Fig. 7 Effect of (**A**) pH and (**B**) H_2O_2 dosage on the degradation activity of $LaFeO_3$/SBA-15 for RhB oxidation. 0.1 g catalyst; 50 mL RhB (0.02 mmol/L)

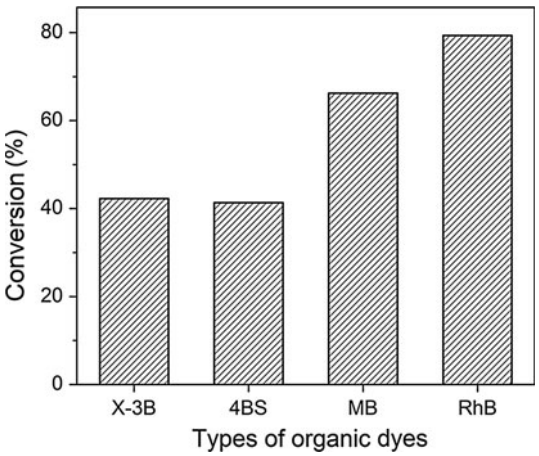

Fig. 8 Catalytic activity of $LaFeO_3$/SBA-15 for various organic dyes, measured at reaction time of 60 min. 0.1 g catalyst; 1 mL H_2O_2 (30 %, w/w); 50 mL dye aqueous solution (0.02 mmol/L)

activity of $LaFeO_3$/SBA-15 for RhB oxidation with the H_2O_2 amount, measured at reaction time of 60 min. The oxidation activity is only 15.0 % in the absence of H_2O_2, but significantly increases when 0.2 mL of H_2O_2 (30 %, w/w) is added to the reaction. The increase is minor with the further increase of H_2O_2 amount. Actually, the oxidation activity is slightly decreased after addition of 0.8 mL of H_2O_2. These results indicate that 0.2 mL of H_2O_2 is adequate for RhB oxidation in this study. Decrease of activity at large amount of H_2O_2 has also been observed and explained in previous literature [42], which supports our results.

In order to check if any Fe^{3+} ions are dissolved during the reaction, acting as homogeneous catalyst for RhB oxidation, we performed atomic absorption spectrometry (Fe lamp, Shimadzu AA-6300) on the filtered aqueous solution after reaction. Results showed that Fe element could not be detected in this measurement, suggesting that Fe^{3+} ion is not dissolved in the reaction or the amount is too low to be detected. Consequently, we consider that $LaFeO_3$/SBA-15 is a very stable and active catalyst for RhB oxidation using H_2O_2 as oxidant.

In addition, we performed high performance liquid chromatography (HPLC, Varian Prostar 210) to check if RhB is degraded after the reaction. 4 mL of aliquots were extracted at different reaction time, i.e., 0 min, 100 min and 120 min, and then subjected to analyze by HPLC. Results showed that one strong peak attributable to RhB appeared at the beginning, but was disappeared at reaction time of 120 min, Figure S4, suggesting that RhB is completely degraded after the reaction. No effort on analyzing the reaction products was tried as their identification is difficult.

In the end, catalytic performances of $LaFeO_3$/SBA-15 for a variety of organic dyes are also investigated, to check its applicability for different dyes. Reactive brilliant red X-3B, direct scarlet 4BS and MB, which are common but important dyes used in industrial plants, were used for study. The concentration of each dye is 0.02 mmol/L. The catalytic tests were done after their adsorption on $LaFeO_3$/SBA-15 reaches equilibrium, similar as that for RhB. Figure 8 shows the oxidation activity of $LaFeO_3$/SBA-15 for the several organic dyes, measured at reaction time of 60 min. The oxidation activity for RhB and MB is 80 and 66 %, respectively, while that for X-3B and 4BS is similar, around 42 %. This indicates that the $LaFeO_3$/SBA-15 is more favorable for catalyzing RhB oxidation. Meanwhile, it also shows considerable activities for other dyes, potentiating its wide applications to different dyes.

4 Conclusions

Supported perovskite oxide, $LaFeO_3$/SBA-15, which combines the advantages of $LaFeO_3$ for catalytic oxidation and mesoporous material SBA-15 for dye adsorption, exhibit large adsorption capacity and high catalytic performances for dye oxidation using H_2O_2 as oxidant. XRD and N_2 physisorption measurements indicate that the catalyst has $LaFeO_3$ perovskite structure and the ordered mesoporous structure of SBA-15 is not destroyed after the deposition of $LaFeO_3$; TEM image shows that the $LaFeO_3$ particles are well dispersed on SBA-15, with particle size of 10–20 nm; while XPS measurement suggests that the main chemical valences of La and Fe are +3 and there have large amounts of oxygen vacancies on the surface. This catalyst is very stable and exhibits high activity for RhB oxidation, and can be reused for at least four times without appreciable loss in the activity. Investigations on the effect of pH value and H_2O_2 amount indicate that the catalyst has wide working pH ranges (from 2 to 10) and 0.2 mL of H_2O_2 (30 %, w/w) is adequate for 50 mL 0.02 mol/L RhB oxidation. Comparative tests on various organic dyes indicate that $LaFeO_3$/SBA-15 is more favorable for RhB oxidation, meanwhile also exhibits considerable activity for other dyes, such as reactive brilliant red X-3B, direct scarlet 4BS and MB, showing promising applications for industrial use.

Acknowledgments Financial supports from the National Science Foundation of China (Grant No. 21203254, 21073238) and the Special Fund of the Central University Research, South-central University for Nationalities (CZZ11007, 12ZNZ006) are gratefully acknowledged.

References

1. Ajmal M, Khan AU (1985) Environ Pollut Ser A. Ecol Biol 37:131
2. Gupta MP, Bhattacharya PK (1985) J Chem Technol Biot 35:23

3. Bhatnagar A, Jain AK (2005) J Colloid Interface Sci 281:49
4. Juang RS, Wu FC, Tseng RL (1997) Environ Technol 18:525
5. Hitz HR, Huber W, Reed RH (1978) J Soc Dyers Colour 94:71
6. Crini G (2003) Bioresour Technol 90:193
7. Al-Qodah Z (2000) Water Res 34:4295
8. Anbia M, Salehi S (2012) Dyes Pigments 94:1
9. Haber F, Weiss J (1934) Proc Roy Soc A 147:332
10. Meriç S, Selcuk H, Gallo M, Belgiorno V (2005) Desalination 173:239
11. Sedlak DL, Andren AW (1991) Environ Sci Technol 25:777
12. Pignatello JJ (1992) Environ Sci Technol 26:944
13. Parra S, Guasaquillo I, Enea O, Mielczarski E, Mielczarki J, Albers P, Kiwi-Minsker L, Kiwi J (2003) J Phys Chem B 107:7026
14. Costa RCC, Lelis MFF, Oliveira LCA, Fabris JD, Ardisson JD, Rios RRVA, Silva CN, Lago RM (2006) J Hazard Mater 129:8
15. Magalhães F, Pereira MC, Botrel SEC, Fabris JD, Macedo WA, Mendonça R, Lago RM, Oliveira LCA (2007) Appl Catal A 332:115
16. Kasiri MB, Aleboyeh H, Aleboyeh A (2008) Appl Catal B 84:9
17. Lv X, Xu Y, Lv K, Zhang G (2005) J Photochem Photobiol A 173:121
18. Luo W, Zhu L, Wang N, Tang H, Cao M, She Y (2010) Environ Sci Technol 44:1786
19. Zhang L, Nie Y, Hu C, Qu J (2012) Appl Catal B 125:418
20. Voorhoeve RJH (1977) Advanced materials in catalysis. Academic Press, New York
21. Zhu JJ, Thomas A (2009) Appl Catal B 92:225
22. Pena MA, Fierro JLG (2001) Chem Rev 101:1981
23. Tejuca LG, Fierro JLG (1993) Properties and applications of perovskite-type oxides. CRC Press, New York
24. Tanaka H, Misono M (2001) Curr Opin Solid State Mater Sci 5:381
25. Zhao DY, Feng JL, Huo QS, Melosh N, Fredrickson GH, Chmelka BF, Stucky GD (1998) Science 279:548
26. Zhao DY, Huo QS, Feng JL, Chmelka BF, Stucky GD (1998) J Am Chem Soc 120:6024
27. Zhu J, Kailasam K, Xie X, Schomaecker R, Thomas A (2011) Chem Mater 23:2062
28. Zhu J, Xie X, Carabineiro SAC, Tavares PB, Figueiredo JL, Schomacker R, Thomas A (2011) Energ Environ Sci 4:2020
29. Liu BS, Wei XN, Zhan YP, Chang RZ, Subhan F, Au CT (2011) Appl Catal B 102:27
30. Li X-K, Ji W-J, Zhao J, Zhang Z-B, Au C-T (2006) J Catal 238:232
31. Liu Y-M, Cao Y, Yan S-R, Dai W-L, Fan K-N (2003) Catal Lett 88:61
32. Galarneau A, Nader M, Guenneau F, Di Renzo F, Gedeon A (2007) J Phys Chem C 111:8268
33. Wei Z-X, Xu Y-Q, Liu H-Y, Hu C-W (2009) J Hazard Mater 165:1056
34. Giraudon JM, Elhachimi A, Wyrwalski F, Siffert S, Aboukaïs A, Lamonier JF, Leclercq G (2007) Appl Catal B 75:157
35. Su H, Jing L, Shi K, Yao C, Fu H (2010) J Nanopart Res 12:967
36. Yang Z, Huang Y, Dong B, Li H-L (2006) Mater Res Bull 41:274
37. Zhao Z, Yang XG, Wu Y (1996) Appl Catal B 8:281
38. Yamazoe N, Teraoka Y, Seiyama T (1981) Chem Lett 10:1767
39. Costa RCC, Lelis MFF, Oliveira LCA, Fabris JD, Ardisson JD, Rios RRVA, Silva CN, Lago RM (2006) J Hazard Mater 129:171
40. Huang CH, Chang KP, Ou HD, Chiang YC, Wang CF (2011) Microporous Mesoporous Mater 141:102
41. Dong YL, Lu B, Zang SY, Zhao JX, Wang XG, Cai QH (2011) J Chem Technol Biot 86:616
42. Merouani S, Hamdaoui O, Saoudi F, Chiha M (2010) Chem Eng J 158:550